Added Value of Dual-Energy Computed Tomography Versus Single-Energy Computed Tomography in Assessing Ferromagnetic Properties of Ballistic Projectiles

Implications for Magnetic Resonance Imaging of Gunshot Victims

Sebastian Winklhofer, MD,† Paul Stolzmann, MD,*† Andreas Meier, MD,† Wolf Schweitzer, MD,* Fabian Morsbach, MD,† Patricia Flach, MD,*† Beat P. Kneubuehl, PhD,‡ Hatem Alkadhi, MD, MPH, EBCR,† Michael Thali, MD, EMBA,* and Thomas Ruder, MD*§*

Objective: The objective of this study was to assess the discriminative power of dual-energy computed tomography (DECT) versus single-energy CT (SECT) to distinguish between ferromagnetic and non–ferromagnetic ballistic projectiles to improve safety regarding magnetic resonance (MR) imaging studies in patients with retained projectiles.

Materials and Methods: Twenty-seven ballistic projectiles including 25 bullets (diameter, 3–15 mm) and 2 shotgun pellets (2 mm each) were examined in an anthropomorphic chest phantom using 128-section dual-source CT. Data acquisition was performed with tube voltages set at 80, 100, 120, and 140 kV(p). Two readers independently assessed CT numbers of the projectile's core on images reconstructed with an extended CT scale. Dual-energy indices (DEIs) were calculated from both 80-/140-kV(p) and 100-/140-kV(p) pairs; receiver operating characteristics curves were fitted to assess ferromagnetic properties by means of CT numbers and DEI.

Results: Nine (33%) of the projectiles were ferromagnetic; 18 were nonferromagnetic (67%). Interreader and intrareader correlations of CT number measurements were excellent (intraclass correlation coefficients, >0.906; $P < 0.001$). The DEI calculated from both 80/140 and 100/140 kV(p) were significantly ($P < 0.05$) different between the ferromagnetic and non–ferromagnetic projectiles. The area under the curve (AUC) was 0.75 and 0.8 for the tube voltage pairs of 80/140 and 100/140 kV(p) ($P < 0.05$; 95% confidence interval, 0.57–0.94 and 0.62–0.97, respectively) to differentiate between the ferromagnetic and non–ferromagnetic ballistic projectiles; which increased to 0.83 and 0.85 when shotgun pellets were excluded from the analysis. The AUC for SECT was 0.69 and 0.73 (80 and 100 kV[p], respectively).

Conclusions: Measurements of DECT combined with an extended CT scale allow for the discrimination of projectiles with non–ferromagnetic from those with ferromagnetic properties in an anthropomorphic chest phantom with a higher AUC compared with SECT. This study indicates that DECT may have the potential to contribute to MR safety and allow for MR imaging of patients with retained projectiles. However, further studies are necessary before this concept may be used to triage clinical patients before MR.

Received for publication April 15, 2013; and accepted for publication, after revision, December 3, 2013.

From the *Department of Forensic Medicine and Radiology, Institute of Forensic Medicine, †Institute of Diagnostic and Interventional Radiology, University Hospital Zurich, Zurich; ‡Department of Forensic Physics and Ballistics, Institute of Forensic Medicine, University of Bern; and §Department of Diagnostic, Interventional and Pediatric Radiology, University Hospital Bern, Bern, Switzerland.

Conflicts of interest and sources of funding: none declared.

Reprints: Sebastian Winklhofer, MD, Institute of Diagnostic and Interventional Radiology, University Hospital Zurich, Raemistrasse 100, 8091 Zurich, Switzerland. E-mail: sebastian.winklhofer@usz.ch.

ISSN: 0020-9996/14/4906–0431

Key Words: MRI safety, computed tomography, dual-energy, material differentiation, ballistics, projectiles, forensic radiology

(*Invest Radiol* 2014;49: 431–437)

Nearly 6000 US soldiers have died of gunshot or shrapnel injuries during their missions in Iraq and Afghanistan.[1,2] In addition, there were more than 74,000 cases of nonfatal and 32,000 cases of fatal firearm injuries within the United States in the year 2011.[3–5] All these cases, both military and civilian, require careful diagnostic and therapeutic workup.

The presence of retained ballistic projectiles or fragments within a patient scheduled for magnetic resonance (MR) imaging represents a challenge to radiologists. Metallic objects located near or in a critical anatomic structure may potentially move because of ferromagnetic interactions with the MR magnet and cause further damage.[6–8]

A recent study illustrates that projectiles containing steel are subject to significant motion, whereas projectiles without steel are to be considered safe for MR.[9] Similar results were reported in several previously published studies.[10,11] Those observations stand in agreement with the ferromagnetic properties of iron, a highly magnetic element that constitutes a major component of steel. It is therefore elementary to assess the composition of a projectile before MR imaging to decide whether it is safe for MR or not. Whereas conventional radiographs are unsuitable for this task, multienergy computed tomography (CT), especially dual-energy CT (DECT), may be able to distinguish between different ballistic materials. The behavior of the individual materials at different energy levels depends on their atomic number, the electron density, their density, and their diameter.[12] Dual-energy CT has become an established tool for characterization of urinary calculi,[13,14] quantification of coronary artery calcium,[15] measurement of contrast agent uptake,[16] or discrimination between contrast media and intracerebral hemorrhage.[17]

Elements with a considerable difference in their atomic number can be characterized with the dual-energy index (DEI).[18,19] This DEI is useful to quantify the dual-energy behavior of materials and might therefore also prove useful to distinguish ballistic projectiles on the basis of their composition.[18]

Ballistic projectiles are usually made from steel, lead, and copper-zinc alloys or a combination of these materials. The 2 most important copper-zinc alloys in projectiles are brass and tombac. The diameter of handgun and rifle bullets and that of pellets range from 2 (shotgun pellets) to 12.7 mm (heavy guns).[20] The main challenge regarding the differentiation of metallic objects is that metals are powerful absorbers of x-rays.[21] Copper plates of less than 1 mm, for

TABLE 1. Characteristics of Projectiles With Respect to Ferromagnetic Versus Non–Ferromagnetic Properties

	Ferromagnetic Properties									Non–Ferromagnetic Properties																	
Diameter, mm	6	6	13	8	8	2	5	9	3	6	15	13	8	2	6	8	9	9	9	9	9	11	12	8	8	8
Material																										
Core	Cu	Cu	Fe	Cu	Cu	Fe	Pb	Cu	Fe	Pb	Pb	Cu	Pb	Pb	Pb	Pb	Cu	Pb	Pb	Pb	Pb	Cu	Pb	Pb	Pb	Pb	Cu
	Ni	Zn		Ni	Zn			Ni				Zn					Zn				Pl	Pl		Cu			Zn
	Pb	Fe		Pb	Fe			Fe																			
Jacket	Fe	Fe		Fe	Fe		Fe			Cu			Cu		Cu	Cu			Cu	Cu	Cu		Cu		Cu	Cu	
										Zn			Zn		Zn	Zn			Zn	Zn	Zn		Zn		Zn	Zn	

Cu indicates copper; Fe, iron; Ni, nickel; Pb, lead; Pl, plastic; Zn, zinc.

example, are used as x-ray filters and lead is used for protective aprons and shields in hospitals.[12] Objects made of metals (such as aluminum, brass, steel, silver, gold, or lead) have the capacity to completely attenuate x-rays and impede even a single x-ray photon from reaching the detector.

Nevertheless, it would be desirable to reliably identify the composition of retained ballistic projectiles or other metallic objects, once detected on plain radiographs, not only in clinical radiology but also in forensic investigations.[21,22] In clinical radiology, this would provide radiologists with a tool to distinguish between patients that are eligible for MR imaging and those who are not.

Goal of the Investigation

The purpose of our study was to investigate the discriminative power of DECT versus single-energy CT (SECT) to differentiate ferromagnetic projectiles from non–ferromagnetic projectiles in an anthropomorphic chest phantom.

MATERIALS AND METHODS

Study Design, Setting, and Projectiles

Twenty-seven contemporary ballistic projectiles including 25 bullets (range of diameter, 3–15 mm) and 2 pellets of different shotguns (pellets size of 2 mm each) were examined in this phantom study. The elemental composition of the projectiles was derived from the manufacturer's specifications. In addition, the authors empirically tested the ferromagnetic properties of each projectile according to the method described by New et al.[23] The projectiles were suspended on a string at the portal of a 3-T MR imaging system (Achieva; Philips Medical Systems, Best, the Netherlands), and their deflection of α greater than 0 degrees from the vertical indicated ferromagnetic properties, which was used as the reference standard. Of the 27 projectiles, 9 (33%) demonstrated marked ferromagnetic properties, whereas 18 were nonferromagnetic (67%). There was no discrepancy between our assessment of the ferromagnetic properties of the projectiles and the manufacturer's specifications. The composition of the projectiles is given in Table 1.

To achieve a realistic and reproducible environment for data acquisition, we used a commercially available, certified anthropomorphic chest phantom (QRM; Quality Assurance in Radiology and Medicine GmbH, Mohrendorf, Germany) in which we placed the projectiles for CT scanning (Fig. 1). The phantom (size, 200 × 300 × 100 mm) consists of a cross-section model of the human chest. It contains artificial lungs and a spine insert surrounded by a shell of soft tissue–equivalent materials and a bore at the position of the mediastinum and heart.[24] The materials were used to build the human tissue–mimicking phantom with regard to density and x-ray attenuation characteristics. The projectiles used in this study were all placed individually in the bore for scanning.

Methods of Measurement

Data acquisition was performed using a 128-section dual-source CT scanner (SOMATOM Definition Flash; Siemens Healthcare, Forchheim, Germany). Tube voltages were set to 80, 100, 120,

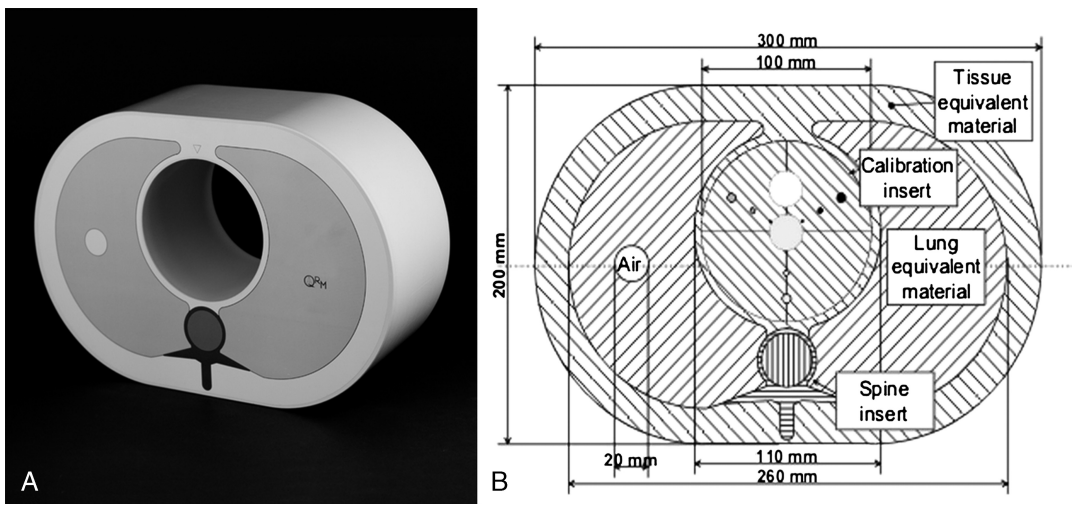

FIGURE 1. Photograph of the anthropomorphic chest phantom (A) with schematic buildup (B).

and 140 kV(p). Scanning parameters were as follows: slice collimation, 2 × 64 × 0.6 mm; slice acquisition, 2 × 128 × 0.6 mm by means of a z-flying focal spot; rotation time, 0.5 seconds; and pitch, 0.6. Tube current-time products were adjusted to yield constancy in CT dose (volume CT dose index = 9.8 mGy) for all scans. Attenuation-based tube current-time modulation (CareDose4D; Siemens Healthcare, Forchheim, Germany) was switched off.

Images were reconstructed from each of the 4 CT acquisitions (ie, 80, 100, 120, and 140 kVp) and each single projectile, resulting in a total number of 44 image sets. Data reconstruction was carried out using a sharp tissue convolution kernel (b70), a slice thickness of 1.5 mm, and a slice increment of 1.0 mm. An extended CT scale was used, which allows for the representation of CT numbers from −1000 to 30,710 Hounsfield units (HUs).[25,26]

Outcomes

Two independent radiologists (R1 and R2, with 4 and 5 years of experience, respectively) who were blinded to the materials and properties of projectiles performed all measurements on an external workstation (Syngo3D, version VA40A, Multi Modality Workplace; Siemens, Forchheim, Germany).

Each CT number measurement of the projectiles was performed 3 times by each reader on independent axial CT images at all 4 tube voltages using the manufacturer's data reading software. Regions of interest (ROIs) were placed in the following:

- *core* defined as the center of the projectile encased by the jacket
- *jacket* defined as the shell around the bullet core

Placement of ROI attempted to avoid areas of inhomogeneity (ie, projectile edges and phantom edges, Fig. 2). From these data, a DEI was calculated according to the following formula[13,18]:

$$DEI = \frac{low\ \ kV(p) - high\ \ kV(p)}{low\ \ kV(p) + high\ \ kV(p)\ \ +\ \ 2000}\ \text{HU}$$

A DEI was calculated for 80- and 140-kV(p) as well as 100- and 140-kV(p) setting (hereafter referred to as dual-energy pairs of 80/140 and 100/140 kV[p]) regarding CT number measurements of the projectile core and jacket. To identify intrareader and interreader variability, measurements were repeated (after a time interval of 2 weeks to avoid recall bias).

Analysis

Continuous variables were expressed as mean (SD); categorical variables, as frequencies and percentages.

The intrareader and interreader agreements regarding CT number measurements of bullets and pellets were analyzed by using intraclass correlation coefficients (ICCs). According to Landis and Koch,[27] ICC values of 0.61 to 0.80 were interpreted as substantial; 0.81 to 1.00, as excellent agreement.

Wilcoxon signed-rank test was used to assess for differences in CT numbers among the different locations of measurements (ie, core, jacket). The non–parametric Friedman test for related samples was used to assess for differences in CT numbers among the different tube voltages (ie, 80, 100, 120, and 140 kV[p]). With regard to 80, 100, 120, and 140 kV(p), CT numbers of projectiles with ferromagnetic properties were compared with those with non–ferromagnetic properties using the nonparametric Mann-Whitney *U* test. This latter test was also used to assess for differences of DEI between projectiles with and without ferromagnetic properties.

Receiver operating characteristics (ROC) analysis was fitted to describe ferromagnetic properties by means of CT numbers and DEI. Point estimates, 95% confidence intervals (CIs), and areas under the ROC curve (AUCs) were calculated.

Statistical analysis was performed using IBM Statistical Package for the Social Sciences statistics software (release 20.0, Chicago, IL). A P value of less than 0.05 was used to denote statistical significance.

RESULTS

Intraobserver and Interobserver Agreement

For intrareader agreement analysis, CT number measurements were significantly correlated ($P < 0.001$ each) with ICCs demonstrating excellent agreement regarding projectiles' cores (R1: ICC, 0.979; R2: ICC, 0.961) and jackets (R1: ICC, 0.925; R2: ICC, 0.951). Hence, mean measurements from both readers were taken for further analysis.

For interreader agreement analysis, CT number measurements of both readers were significantly correlated ($P < 0.001$ each) with each other. The ICCs demonstrated excellent agreements regarding CT number measurements of projectiles' cores (ICC, 0.969) and jackets (ICC, 0.906).

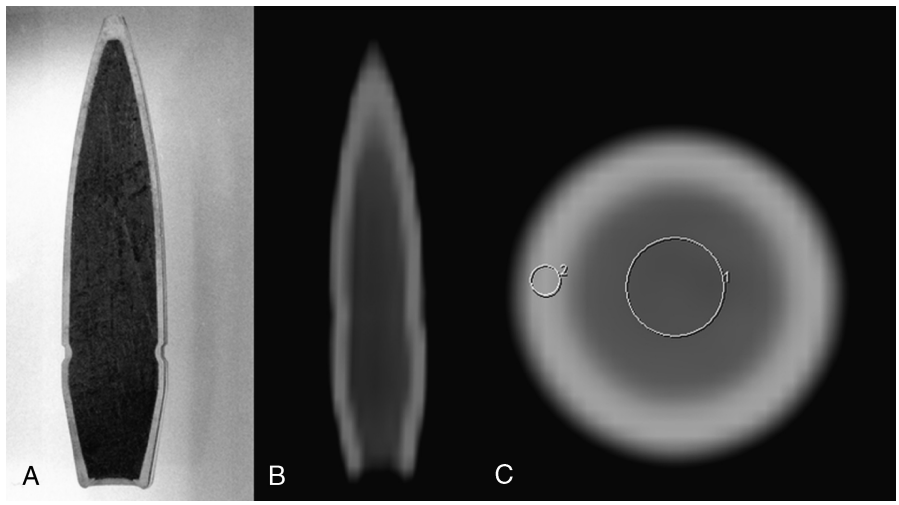

FIGURE 2. Exemplary photograph (A) and corresponding CT image (B) of a jacketed bullet (7.5 × 5.5 GP 11; 7.5-mm diameter). The ROIs were placed in axial slices (C) in the jacket and the core of the projectiles.

TABLE 2. Single-Energy CT Number of Projectiles as Obtained in the Core and Jacket With Respect to the Different Tube Voltages of Data Acquisition

	80 kV(p)		100 kV(p)		120 kV(p)		140 kV(p)	
Single-Energy	**Core**	**Jacket**	**Core**	**Jacket**	**Core**	**Jacket**	**Core**	**Jacket**
Ferromagnetic								
Mean (SD) CT number, HU	18561 (7157)	29803 (1233)	19657 (6198)	29305 (2209)	20216 (5522)	28472 (3163)	20043 (5621)	28068 (4150)
Minimum, HU	8887	27440	12624	24493	12690	22125	12001	19355
Maximum, HU	30622	30709	30707	30707	30708	30703	30708	30696
Nonferromagnetic								
Mean (SD) CT number, HU	13596 (4880)	28856 (1641)	14823 (5147)	29309 (1262)	16690 (4987)	29204 (1487)	16966 (5162)	28796 (2005)
Minimum, HU	5346	24708	9028	26167	3593	26273	3593	24184
Maximum, HU	28715	30592	28627	30701	27771	30647	28890	30627

CT indicates computed tomography; HU, Hounsfield unit.

Single-Energy Analysis

Measurements of CT number differed significantly between the core and jacket with all tube voltage settings (80, 100, 120, and 140 kV[p]; each $P < 0.01$). Thus, subsequent data analysis was performed for each of the locations of core and jacket separately. The CT numbers of the core ($P < 0.05$) were significantly different at different tube voltage levels (ie, 80, 100, 120, and 140 kV[p]), whereas the CT numbers of jacket ($P = 0.42$) yielded no statistically significant difference at different tube voltages.

Table 2 demonstrates the results of CT number measurements with respect to the acquisitions at 80, 100, 120, and 140 kV(p). In 30% of all projectiles, the measured CT number in the jacket almost reached, reached, or probably even exceeded the extended CT scale upper limit of 30,700 HU. Therefore, we excluded all measurements in the jacket for further statistical calculations.

For the comparison of ferromagnetic versus non–ferromagnetic projectiles, no significant differences were found regarding CT numbers of the projectiles' core at 120 and 140 kV(p) ($P = 0.136$ and $P = 0.169$, respectively), whereas 80 and 100 kV(p) demonstrated significant differences ($P = 0.036$ and $P = 0.017$, respectively). The AUC was 0.69 for the 80-kV(p) measurements (95% CI: 0.400, 0.975) and 0.73 for the 100-kV(p) measurements (95% CI: 0.517, 0.948). The AUC increased to 0.76 (95% CI: 0.517, 0.999) for 80 kV(p) and 0.79 (95% CI: 0.608, 0.976) for 100 kV(p) when only bullets (ie, after exclusion of pellets) were included in the analysis.

Dual-Energy Analysis

Regarding CT number measurements in the core of the projectile, the overall mean (SD) DEIs (including ferromagnetic and non–ferromagnetic projectiles) calculated from 80/140 and 100/140 kV(p) were −0.06 (0.09) (range, −0.18 to 0.28) and −0.04 (0.06) (range, −0.16 to 0.07), respectively (Table 3).

Dual-energy indices as derived from CT numbers measurements in the core of ferromagnetic projectiles were significantly ($P < 0.05$, both dual-energy pairs) higher than those of non–ferromagnetic ones. Concerning non–ferromagnetic projectiles, mean (SD) DEI was −0.07 (0.09) (range, −0.18 to 0.28) for the dual-energy pair of 80/140 kV(p) and was −0.06 (0.05) (range, −0.16 to −0.06) for the dual-energy pair of 100/140 kV(p). Regarding projectiles with ferromagnetic properties, mean (SD) DEI was −0.03 (0.06) (range, −0.10 to 0.07) for the dual-energy pair of 80/140 kV(p) and was −0.01 (0.05) (range, −0.07 to 0.07) for the dual-energy pair of 100/140 kV(p). Figures 3 and 4 demonstrate a high- versus low-voltage CT number diagram and DEI as derived from core CT

TABLE 3. Dual-Energy Index of Projectile's Core With Respect to the Different Tube Voltage Pairs

Dual-Energy Pairs	**80/140 kV(p)**	**100/140 kV(p)**
Mean DEI	−0.056	−0.044
SD	0.085	0.056
Minimum	−0.18	−0.16
Maximum	0.28	0.07
P	**<0.05**	**<0.05**

P values are given for the comparison of DEI between ferromagnetic and non–ferromagnetic projectiles. Significant differences (printed in boldface, Mann-Whitney *U* test) were found regarding the DEI of the projectile's core derived from dual-energy pair of either 80/140 or 100/140 kV(p).

DEI indicates dual-energy index.

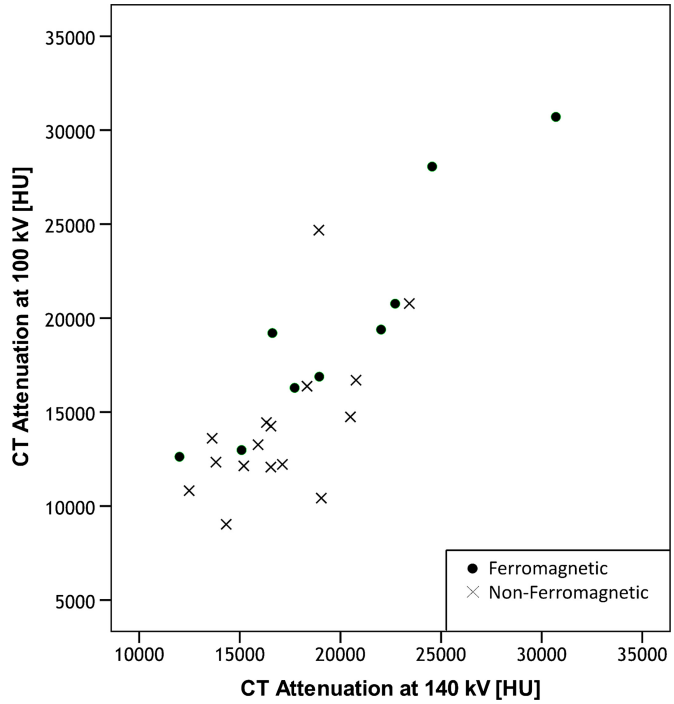

FIGURE 3. High- versus low-voltage CT number diagram for the data acquisition with 100 kV and 140 kV [HU]. Symbols indicate the different ferromagnetic properties with ferromagnetic versus non-ferromagnetic projectiles.

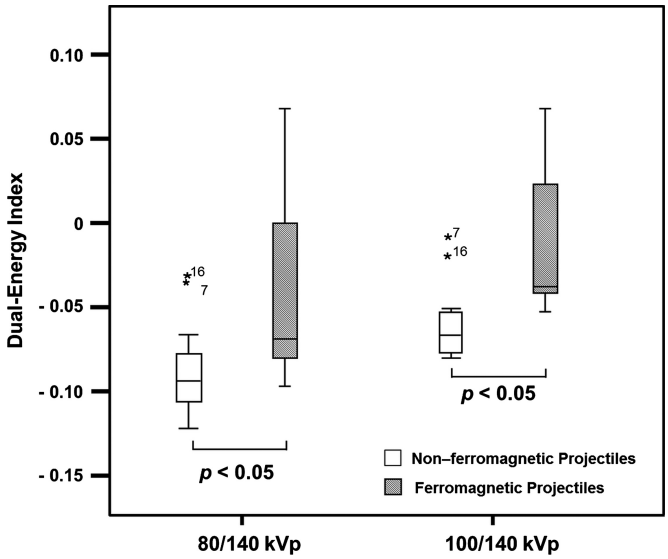

FIGURE 4. Box plot demonstrating the DEI as derived from core CT number measurements of projectiles with non–ferromagnetic (empty boxes) and ferromagnetic properties (striped pattern) regarding dual-energy pairs of both 80/140 and 100/140 kV(p). The DEI of non–ferromagnetic projectiles was significantly ($P < 0.05$) lower as compared with ferromagnetic projectiles for both dual-energy pairs.

number measurements according to projectiles with ferromagnetic and non–ferromagnetic properties of both dual-energy pairs.

The ROC analysis revealed a significant ($P < 0.05$ each) discriminative power of DEI derived from core CT numbers to differentiate between ferromagnetic and non–ferromagnetic projectiles for both tube-voltage pairs. The AUC was 0.75 (95% CI: 0.565, 0.941) for 80/140 kV(p) and 0.80 (95% CI: 0.620, 0.973) for 100/140 kV(p) (Fig. 5). The AUC ($P < 0.05$ each) increased to 0.83 (95% CI: 0.657, 0.995) for 80/140 kV(p) and 0.85 (95% CI: 0.696, 1.000) for 100/140 kV(p) when only bullets (ie, after exclusion of pellets) were included in the analysis.

DISCUSSION

Our study demonstrates that DECT is more suitable than SECT to distinguish ferromagnetic from non–ferromagnetic projectiles in an anthropomorphic model at extended CT scale.

The high intrareader and interreader reliability regarding CT number measurement stands in agreement with the findings from other studies comparing the reliability of ROI measurements and further fortifies this established method to quantify x-ray attenuation on CT images.[21,28,29] Therefore, we believe that the used technique for ROI drawing is adequate and reliable and that, in daily routine, no repeated measurements or second readouts would be required.

Our results indicate that DEI is a suitable method to quantify the dual-energy behavior of ferromagnetic and non–ferromagnetic projectiles. This finding concurs with both the theoretical principle of the DEI and the results from previous studies where DEI was used to distinguish between materials.[13,18,28]

Dual-energy analyses are based in part on the differentiation of low *Z*-number from high *Z*-number elements. Therein, 2 main mechanisms contribute to the CT attenuation. The first mechanism is represented by the photoelectric effect that predominates at lower photon energies and is heavily dependent on energy. Compton scattering occurs almost independently of the photon energy. The photoelectric effect is related to high atomic numbers, whereas the Compton scattering is predominantly related to the density of the material.[19,30]

The AUC for the dual-energy–based differentiation of ferromagnetic projectiles from those without non–ferromagnetic properties as approached herein was 0.75 and 0.8 for the dual-energy pairs of 80/140 and 100/140 kV(p), with the latter increasing to 0.85 when shotgun pellets were excluded. Compared with this, the AUC for SECT analysis with 80 and 100 kV(p) demonstrated markedly lower results for both energies.

We believe that the inclusion of pellets reduced the AUC and, therefore, the discriminative power because of partial volume artifacts that may have induced a non–systematic error.[31] This hypothesis is supported by the fact that CT numbers of the jacket did not allow for the discrimination of magnetic properties of the projectile. The extended CT-scale upper limit of 30710 was reached, almost reached, or probably exceeded in numerous cases of the measurements of the jacket (30%). Thus, the location of ROI placement seems to play an important role.

The findings of this model study provide evidence that DECT is capable to differentiate ferromagnetic projectiles from non–ferromagnetic projectiles with a higher degree of certainty than SECT is. The difference between DECT and SECT can be explained by the fact that x-ray attenuation depends not only on absorber characteristics (such as electron density and atomic number) but also on x-ray beam characteristics. Previous studies on this topic revealed that the CT values of high-density absorbers will vary significantly if scanned with different CT scanners (despite using the same scan parameters).[21] The reason for this is that the composition of a standard polychromatic x-ray beam varies between CT manufacturers, between different generations of scanners from the same manufacturer, and, finally, on the age of the x-ray tube. This means that the actual Hounsfield unit values of the ferromagnetic and non–ferromagnetic projectiles as presented in Table 2 are not necessarily reproducible on a different scanner. They should therefore not be regarded as reference values that allow for a distinction between ferromagnetic and non–ferromagnetic projectiles. The ratio between x-ray attenuation at low and high kilovolt (peak), however, is less vulnerable to interscanner discrepancies. Therefore, the DEI is of

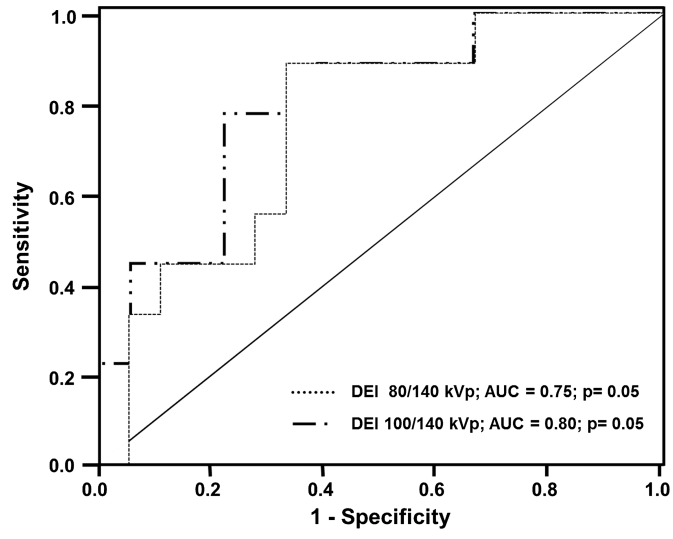

FIGURE 5. Receiver operating characteristics curves for DEIs derived from core CT number measurements for tube voltage pairs of 80/140 and 100/140 kV(p) versus ferromagnetic properties of the projectiles.

more practical use than individual HU values from SECT. Currently, patients with retained non–medical metallic objects such as projectiles are usually precluded from MR imaging. However, not all of these objects do have ferromagnetic properties. This means that a fraction of patients with retained metallic objects may, in fact, be eligible for elective MR studies. It is conceivable that focused DECT analysis of radiologically proven metallic objects can be performed to triage patients for MR imaging in the future. It is important to note that it is yet too early to use this method on actual patients with retained ballistic projectiles and that the calculated AUC might be too low to be useful.

However, if our preliminary results can be validated in future prospective studies in different phantoms, in different surroundings, or in ex vivo studies, our findings may have an impact on MR safety rules and regulations.

Furthermore, our study does not investigate into potential tissue damage by induced voltage and/or heating of projectiles, but it was shown that heating is minimal and likely clinically insignificant.[9]

Limitations

Several limitations of this study deserve comment. However, before discussing these limitations, it is important to recall the objective of this feasibility study: to test whether DECT is able to distinguish between ferromagnetic and non–ferromagnetic projectiles. Currently, there are numerous hurdles between the innovation and potential application of this method in clinical routine. Factors such as relative position of the projectile within a patient (and within the gantry), anatomic structures adjacent to the projectile, orientation of the projectile in the scanner, artifacts (notably beam hardening and photon starvation), and interscanner variability are not yet accounted for. These critical parameters must be assessed systematically and separately before this method should be considered for application in living patients.

There is no doubt that artifacts such as beam hardening, scatter, and photon starvation contaminate the attenuation measurements in any metallic object.[21] This represents a challenge for DEI calculation: the DEI values in this study, which were all calculated from "contaminated" CT numbers, were lower than the theoretical DEI values (eg, pure iron should have a DEI of approximately 0.3). However, this systematic error is currently insurmountable because x-ray attenuation as measured through CT numbers inevitably includes a certain contamination from artifacts, especially in (both ferromagnetic and nonferromagnetic) metals. Nevertheless, the results of this study suggest that this contamination does not preclude DECT-based distinction between ferromagnetic and non–ferromagnetic projectiles.

It is important to discuss the fact that measurements on the jackets proved to be unhelpful in distinguishing between projectiles with and without iron. This limitation may seem critical in projectiles with metal jackets. However, in the projectiles used in this study (including those with metal jackets), measurements of the core were sufficient to distinguish between ferromagnetic and non–ferromagnetic properties. This finding indicates that the presence (or absence) of iron in the jacket is sufficient to affect the x-ray attenuation in the core of a projectile and thereby contributes to the distinction between ferromagnetic and non–ferromagnetic properties.

This study was further limited by the relatively small sample size; a larger sample would certainly have increased the statistical power. However, the number of projectiles was sufficient to demonstrate technical feasibility of the research concept and the selection of projectile covers a wide range and variety of different projectile types.

One final word of caution: It is important to remember that the results from this model study are not directly applicable to living patients. Notably, the influence of position and orientation of a projectile within a patient will affect HU measurements. In addition, one should keep in mind that these results from unused, intact commercial projectiles are not necessarily transferable to shrapnel from self-made explosive devices or similar custom-made projectiles.

However, the authors hope to investigate the previously mentioned technical challenges related to projectiles size and image artifacts on material decomposition and projectile identification in a future study.

Despite all current technical challenges, DECT has the technical ability to distinguish between ferromagnetic and non–ferromagnetic projectiles. This preliminary model study indicates that DECT scans at extended CT scale may offer (at some point in the future) a tool to differentiate patients who are eligible for MR (despite the presence of retained metallic objects) from those who are not eligible for MR. Thereby, this method may contribute to MR safety. However, further studies are necessary before this concept may be used to triage clinical patients for MR.

REFERENCES

1. Gerhardt RT, De Lorenzo RA, Oliver J, et al. Out-of-hospital combat casualty care in the current war in Iraq. *Ann Emerg Med*. 2009;53:169–174.
2. Defense USDo. Global War on Terrorism, October 7, 2001 Through May 7, 2012 DoD Personnel & Procurement Reports and Data Files. Available at: http://siadapp.dmdc.osd.mil/personnel/CASUALTY/gwot_reason.pdf. Accessed May 7, 2012.
3. Centers for Disease Control and Prevention NCfIPaCW-bISQaRSW. 2013. Available at: http://www.cdc.gov/injury/wisqars/index.html. Accessed March, 17, 2013.
4. Hoyert DL, Xu J. Deaths: preliminary data for 2011. *Natl Vital Stat Rep*. 2012;61:19.
5. Ranney ML, Sankoff J, Newman DH, et al. A call to action: firearms, public health, and emergency medicine. *Ann Emerg Med*. 2013;61:700–702.
6. Eshed I, Kushnir T, Shabshin N, et al. Is magnetic resonance imaging safe for patients with retained metal fragments from combat and terrorist attacks? *Acta Radiol*. 2010;51:170–174.
7. Smugar SS, Schweitzer ME, Hume E. MRI in patients with intraspinal bullets. *J Magn Reson Imaging*. 1999;9:151–153.
8. Stecco A, Saponaro A, Carriero A. Patient safety issues in magnetic resonance imaging: state of the art. *Radiol Med*. 2007;112:491–508.
9. Dedini RD, Karacozoff AM, Shellock FG, et al. MRI issues for ballistic objects: information obtained at 1.5-, 3- and 7-Tesla. *Spine J*. 2013;13:815–822.
10. Teitelbaum GP, Yee CA, Van Horn DD, et al. Metallic ballistic fragments: MR imaging safety and artifacts. *Radiology*. 1990;175:855–859.
11. Shellock FG, Morisoli S, Kanal E. MR procedures and biomedical implants, materials, and devices: 1993 update. *Radiology*. 1993;189:587–599.
12. Weissleder R. *Primer of Diagnostic Imaging*. 4th ed. Philadelphia, PA: Mosby Elsevier; 2007:696–700.
13. Graser A, Johnson TR, Bader M, et al. Dual energy CT characterization of urinary calculi: initial in vitro and clinical experience. *Invest Radiol*. 2008;43:112–119.
14. Thomas C, Krauss B, Ketelsen D, et al. Differentiation of urinary calculi with dual energy CT: effect of spectral shaping by high energy tin filtration. *Invest Radiol*. 2010;45:393–398.
15. Schwarz F, Nance JW Jr, Ruzsics B, et al. Quantification of coronary artery calcium on the basis of dual-energy coronary CT angiography. *Radiology*. 2012;264:700–707.
16. Feuerlein S, Heye TJ, Bashir MR, et al. Iodine quantification using dual-energy multidetector computed tomography imaging: phantom study assessing the impact of iterative reconstruction schemes and patient habitus on accuracy. *Invest Radiol*. 2012;47:656–661.
17. Gupta R, Phan CM, Leidecker C, et al. Evaluation of dual-energy CT for differentiating intracerebral hemorrhage from iodinated contrast material staining. *Radiology*. 2010;257:205–211.
18. Krauss B, Schmidt B, Flohr TG. Dual source CT. In: Johnson TRC, Fink C, Schönberg SO, Reiser MF, eds. *Dual Energy CT in Clinical Practice*. Heidelberg, Germany: Springer; 2011:11–20.
19. Johnson TRC, Kalender WA. Physical Background. In: Johnson TRC, Fink C, Schönberg SO, Reiser MF, eds. *Dual Energy CT in Clinical Practice*. Berlin, Germany: Springer; 2011:3–9.
20. Kneubuehl BP. *Wound Ballistics Basics and Applications*. Berlin, Germany: Springer; 2011:47.
21. Ruder TD, Thali Y, Schindera ST, et al. How reliable are Hounsfield-unit measurements in forensic radiology? *Forensic Sci Int*. 2012;220:219–223.

22. Bolliger SA, Oesterhelweg L, Spendlove D, et al. Is differentiation of frequently encountered foreign bodies in corpses possible by Hounsfield density measurement? *J Forensic Sci*. 2009;54:1119–1122.
23. New PF, Rosen BR, Brady TJ, et al. Potential hazards and artifacts of ferromagnetic and nonferromagnetic surgical and dental materials and devices in nuclear magnetic resonance imaging. *Radiology.* 1983;147:139–148.
24. Ulzheimer S, Kalender WA. Assessment of calcium scoring performance in cardiac computed tomography. *Eur Radiol*. 2003;13:484–497.
25. Jackowski C, Lussi A, Classens M, et al. Extended CT scale overcomes restoration caused streak artifacts for dental identification in CT—3D color encoded automatic discrimination of dental restorations. *J Comput Assist Tomogr*. 2006;30:510–513.
26. Woisetschlager M, Lussi A, Persson A, et al. Fire victim identification by postmortem dental CT: radiologic evaluation of restorative materials after exposure to high temperatures. *Eur J Radiol*. 2011;80:432–440.
27. Landis JR, Koch GG. The measurement of observer agreement for categorical data. *Biometrics*. 1977;33:159–174.
28. Stolzmann P, Kozomara M, Chuck N, et al. In vivo identification of uric acid stones with dual-energy CT: diagnostic performance evaluation in patients. *Abdom Imaging*. 2010;35:629–635.
29. Boll DT, Patil NA, Paulson EK, et al. Focal cystic high-attenuation lesions: characterization in renal phantom by using photon-counting spectral CT–improved differentiation of lesion composition. *Radiology.* 2010;254: 270–276.
30. Fornaro J, Leschka S, Hibbeln D, et al. Dual- and multi-energy CT: approach to functional imaging. *Insights Imaging*. 2011;2:149–159.
31. Stolzmann P, Scheffel H, Rentsch K, et al. Dual-energy computed tomography for the differentiation of uric acid stones: ex vivo performance evaluation. *Urol Res*. 2008;36:133–138.